Microscopic structural changes during photodegradation of low-density polyethylene detected by Raman spectroscopy

Microscopic structural changes during photodegradation of low-density polyethylene detected by Raman spectroscopy

Yusuke Hiejima, Takumitsu Kida, Kento Takeda, Toshio Igarashi and Koh-hei Nitta*

Department of Chemical and Materials Science, Kanazawa University, Kakuma Campus, Kanazawa 920-1192, Japan

*Corresponding author: Koh-hei Nitta (E-mail: nitta@se.kanazawa-u.ac.jp)

Abstract

Raman spectroscopy has been used to reveal the microscopic structural changes of low-density polyethylene under ultraviolet irradiation. The fraction of non-crystalline consecutive trans chains (the molecular chains in the trans conformation separate from the orthorhombic crystalline phase) drastically decreases at ~600 h, together with a decrement in the molecular weight and an increment in the crystallinity owing to chemicrystallization. This suggests that short trans chains are prolonged to form consecutive trans chains before chemicrystallization. Moreover, gradual increases of the stretching and compression stresses are observed on the trans and amorphous chains,

respectively. These conformational changes are detected by Raman spectroscopy even in the early stage of photodegradation. Chemicrystallization at ~600 h is accompanied by structural changes, such as shortening of the interchain distance of the lamellar crystals and thinning of the amorphous layer, which induce formation of surface cracks on the macroscopic specimen.

Keywords: Raman spectroscopy; Photodegradation; Low-density polyethylene; Chemicrystallization

1. Introduction

Degradation of polymeric materials is induced by various environmental factors, such as sunlight, heat, and humidity, which result in deterioration of the physical properties, such as the color change, gloss, and impact strength. The chemical aspects of the degradation processes [1] and the stabilization mechanisms [2,3] have been intensively investigated [4]. The mechanism of deterioration of these physical properties during degradation in various environments has also been discussed [5–14]. For example, because of the growing importance of low-density polyethylene (LDPE) in the

agricultural industry, degradation and stabilization of LDPE have been intensively investigated [15,16] based on standard testing methods [17]. However, the molecular mechanisms that induce modification of the hierarchical structures are still unclear.

It has been demonstrated that degradation of polymeric materials is accompanied by structural and morphological changes at various levels [9-12]. Chemical modifications of the polymer chains such as chains scission, branching and crosslinking, as well as formation of carbonyl groups owing to oxidation, are also accompanied by appreciable changes in the superstructures such as the increase of crystallinity [18] and decrease of the amorphous thickness. Although the relation of these structural modifications to the deterioration of the mechanical properties such as the drastic decrease of the toughness has been investigated, a clear correlation has not been established yet [10].

Spectroscopic techniques are used to evaluate the molecular and structural changes of polymeric systems during degradation. Infrared absorption spectroscopy has been extensively applied to evaluate degradation [19,20]. The carbonyl index [21], which is the relative intensity of the absorption of the C=O stretching mode at ~1700 cm^{-1}, is

used as a measure of degradation caused by oxidation reactions [22,23]. The limitations of using the carbonyl index to predict physical deterioration have been recently discussed [24]. Raman spectroscopy has also been used to investigate degradation of polyethylene (PE) and PE blends [25,26]. The increase in the crystallinity of photodegraded PE has been measured by Raman spectroscopy [27]. Ultra-high molecular-weight PE is used for biomedical purposes, such as artificial bones and joints [26,28]. Its physical and chemical characteristics, such as the crystallinity and degree of oxidation, have been evaluated by Raman spectroscopy [29-32].

In this work, we applied Raman spectroscopy for photodegradation of LDPE, and found that the Raman spectral shifts, as well as the intensities, are useful to provide structural insight into photodegradation of LDPE. Spectroscopic analysis revealed the microscopic structural changes during photodegradation, including in the early stage before the onset of chemicrystallization.

2. Materials and methods

LDPE (Prime Polymer Co., Ltd.) with a density of 0.92 g/cm^3 and a melt index of 4

g/10 min was used in this study. We have confirmed that the LDPE contained 0.2 wt.% of dibutylhydroxytoluene as the antioxidant. To simulate the rotational molding process, LDPE sheets with a thickness of 0.5 mm were prepared as follows. LDPE powder was preheated in a hot press at 150 °C for 3 min and then degassed at 150 °C for 2 min. The sample was pressurized at 10 MPa for 1 min. The sample was then heated to 200 °C in 8 min and gradually cooled to 180 °C in 8 min, followed by quenching to room temperature.

The photodegraded LDPE sheets were prepared with a Xenon Weather Meter (SX2-75, Suga Test Instruments). A Xenon fade lamp was used as the light source. The LDPE sheets were irradiated at 60 W/m^2 in the wavelength range 300–400 nm at a black panel temperature of 89 °C under the no rain condition. Note that the present condition has recently been employed for interior components of automobiles, in accordance with increasing demands for harsh conditions such as in the desert area. The irradiation time was set at 120 to 1200 h.

High-temperature gel permeation chromatography (HT-GPC) was performed at 140 °C using a Viscotek Triple Detector HT-GPC (Model-SG system, Malvern

Instruments Ltd., Worcestershire, UK) containing refractive index, light scattering, and viscometer detectors. *o*-Dichlorobenzene with 0.05% butylated hydroxytoluene as an anti-oxidant was used as the solvent. The samples were dissolved at 140 °C to obtain a concentration of 1.0 mg/ml. A polystyrene standard sample was used for column calibration.

A Raman spectrometer previously applied to rheo-Raman measurements [33,34] was used. A DPSS laser (RLK-640-200, LASOS) and a CCD camera equipped with a monochromator (PIXIS100 and SpectraPro 2300i, Princeton Instruments) were used as the light source and detector, respectively. Each Raman spectrum was accumulated 20 times with an exposure time of 2 s. The Raman spectrum was fitted with the sum of Voigt functions using the nonlinear Levenberg–Marquardt method, and the peak positions and areas were determined. The uncertainty of the peak positions and areas for the Raman bands were less than ±0.32 cm^{-1} and ±6.2%, respectively, except for the 1080 cm^{-1} band (±10% uncertainty for the peak area).

The peak shift of each Raman band $\Delta\nu$ is defined as the deviation of the peak position during ultraviolet (UV) irradiation:

$$\Delta\nu = \nu(t) - \nu(0), \quad (1)$$

where $\nu(0)$ and $\nu(t)$ are the peak positions before and after irradiation.

The Raman bands at 1298 and 1305 cm^{-1} are assigned to the CH_2 twisting modes of the trans and amorphous conformers, respectively (Table 1). It has been suggested that 3–5 consecutive trans chains contribute to the intensity of the Raman band at 1298 cm^{-1} [35]. Therefore, the mass fractions of the trans and amorphous conformers were determined using the following equations [36,37]:

$$\chi_t = \frac{I_{1298}}{I_{1298} + I_{1305}}, \quad (2)$$

$$\chi_a = \frac{I_{1305}}{I_{1298} + I_{1305}} \quad (3)$$

where I_{1298} and I_{1305} are the intensities of the Raman bands at 1298 and 1305 cm^{-1}, respectively. It is noted that the CH_2 twisting modes at 1298 and 1305 cm^{-1} were used as the internal reference [36]; the peak position of the prominent peak at 1298 cm^{-1} was assumed to be unchanged, and the intensity of each Raman band was determined as its peak area divided by the sum of the peak areas of two CH_2 twisting bands at 1298 and 1305 cm^{-1}. Using the intensity of the Raman band at 1418 cm^{-1} assigned to the orthorhombic crystalline chains, the orthorhombic crystallinity was determined by [36]

$$\chi_c = \frac{I_{1418}}{A\left(I_{1298} + I_{1305}\right)}, \tag{4}$$

where A (=0.46) is the experimental constant. It has been found that PE has an intermediate phase composed of amorphous trans chains separate from the orthorhombic crystals [36,38]. The fraction of the non-crystalline consecutive trans (NCCT) chains was determined by [37]

$$\chi_{NCCT} = \chi_t - \chi_c . \tag{5}$$

3. Results and discussion

Photographs of the LDPE specimens before and after the UV exposure tests are shown in Fig. 1. While the LDPE specimen is semi-transparent before UV irradiation, the transparency of the specimen decreases with increasing exposure time and the color becomes yellowish. From the optical microscopic images shown in Fig. 1(b), onset of crack formation is observed at 840 h. After 1080 h, surface cracks have propagated over the entire specimen. These macroscopic changes are commonly observed during the decrease of the gloss and the increase of the yellowness index, both of which are conventionally used as an indicator of polymeric material degradation.

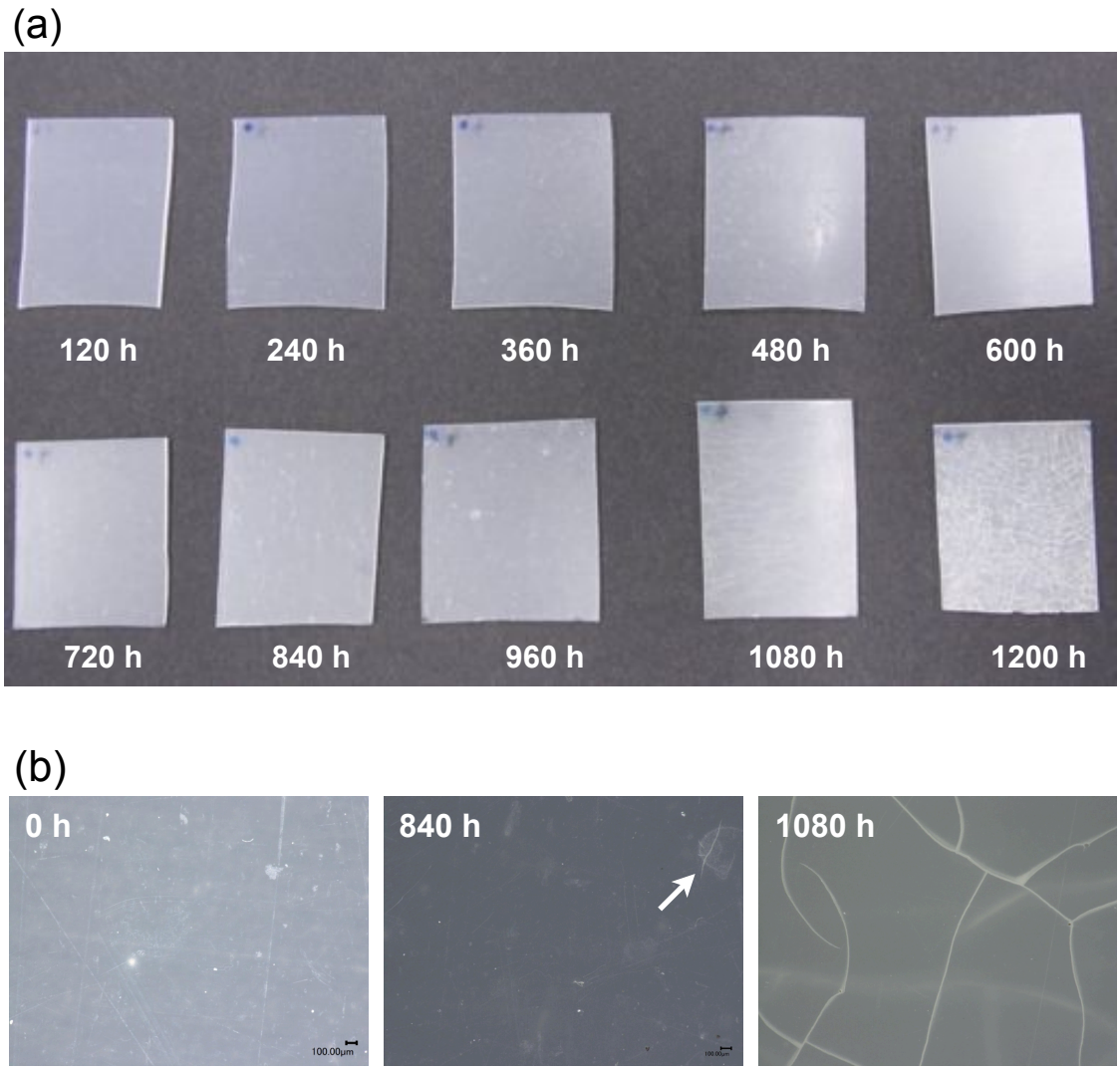

Fig. 1 (a) Macroscopic and (b) microscopic images of the LDPE sheets before and after UV irradiation. The exposure times are shown in the figures. The arrow denotes the onset of surface crack formation.

GPC traces and intrinsic viscosities of LDPE at various exposure times are shown in Fig. 2. The molecular weight distributions are slightly broadened in the early stage of

the photodegradation process up to 480 h, followed by an abrupt decrease of the molecular weight at 600 h indicative of scission of PE chains [9]. The lower shift of intrinsic viscosity with the exposure time suggests modification of chains structure such as the formation of branches and crosslinks. The slope in the low molecular weight region becomes more gradual after UV irradiation compared to those in the high molecular weight region, suggesting that short chains are more likely to be modified during photodegradation.

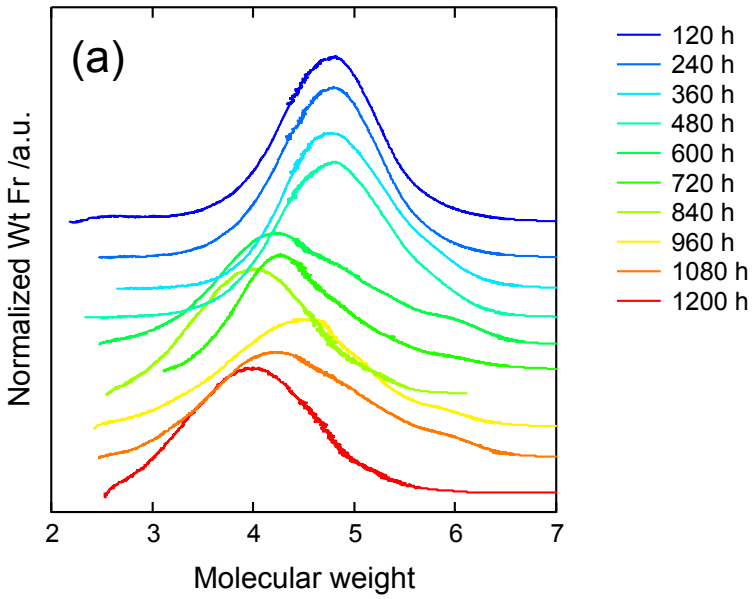

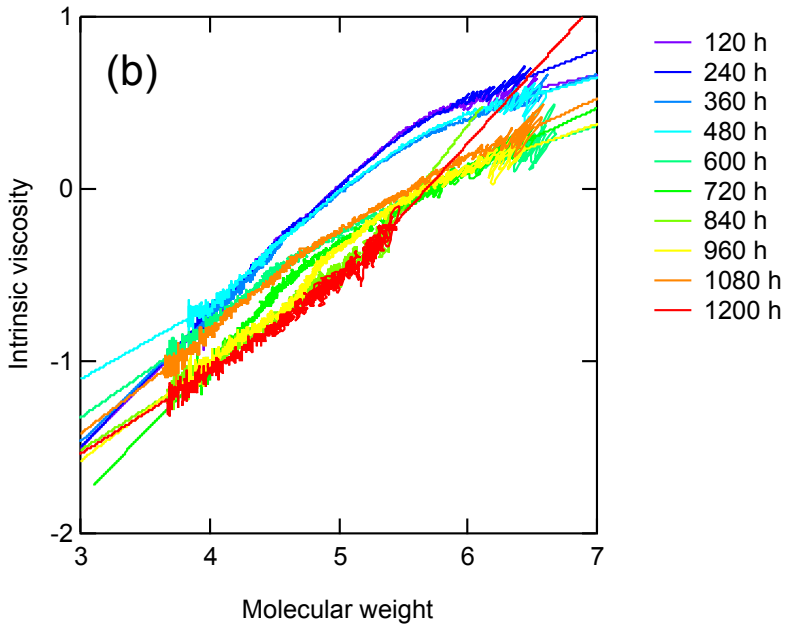

Fig. 2 (a) GPC traces and (b) intrinsic viscosities of LDPE at various UV exposure times.

The Raman spectra of photodegraded LDPE at various exposure times are shown in Fig. 3. The assignments of the Raman bands of PE are listed in Table 1. The intensities of the Raman spectra were normalized by the intensity of the CH_2 twisting bands at 1298 and 1305 cm^{-1} [39,40]. The intensity of the broad 1080 cm^{-1} band assigned to the C–C stretching mode of the amorphous chains gradually decreases with increasing irradiation time, indicating an increase in the crystallinity. A similar decrease in the intensity of the amorphous band is observed in high-density polyethylene (HDPE) exposed in an aqueous solution of a surfactant [41]. The peak positions and areas of the

crystalline C–C stretching modes at 1063 and 1130 cm^{-1} slightly vary with the irradiation time. The spectral changes are more obvious in the 1400 cm^{-1} region, as shown in Fig. 2(b). The crystalline (1418 cm^{-1}) and amorphous (1460 cm^{-1}) bands show clear red and blue shifts, respectively. Similar spectral changes have been observed during environmental stress cracking [30]. Although no obvious Raman peak is observed in the 1700 cm^{-1} range, the formation of carbonyl group on the surface is confirmed by the attenuated total reflection infrared (ATR-IR) spectra as shown in S-7. The variation of the peak areas and positions will be discussed in the following paragraphs.

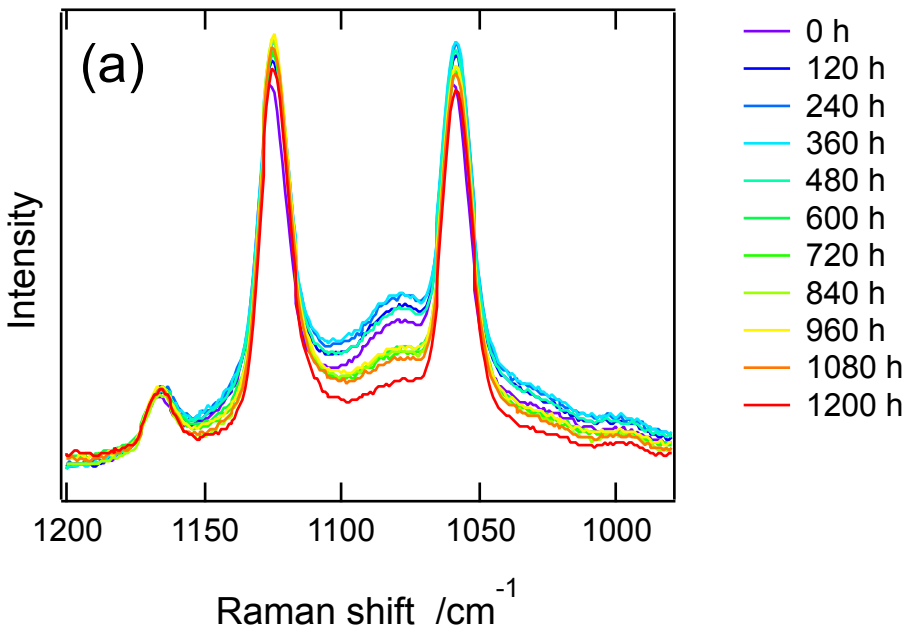

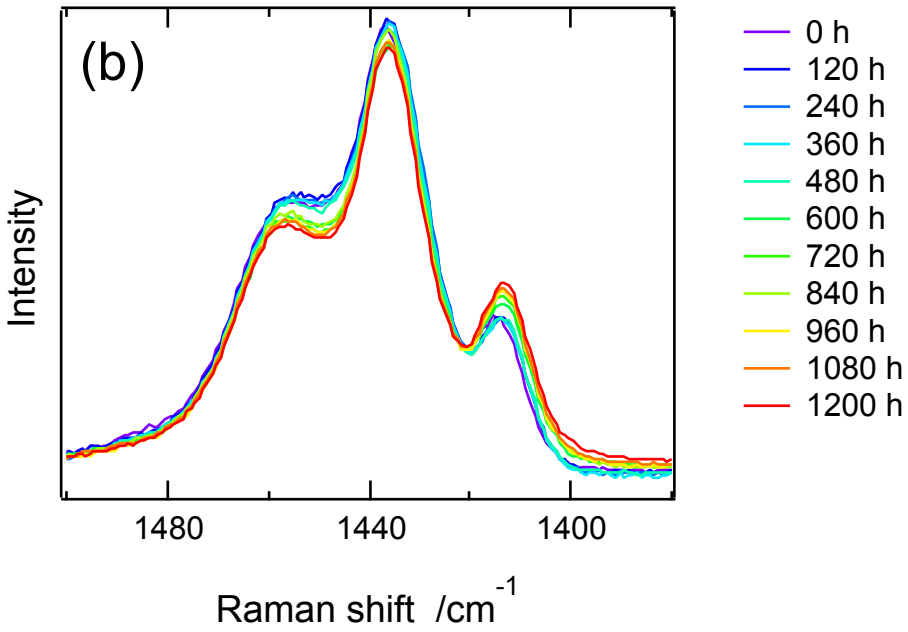

Fig. 3 Raman spectra of LDPE after UV exposure tests at various irradiation times in the (a) 1100 and (b) 1450 cm^{-1} regions.

Table 1 Vibrational modes and phase assignments of the Raman bands of PE [42-45]

Peak position /cm^{-1}	Vibrational mode [a)]	Phase
1063	ν_{as} (C-C)	Trans chain
1080	ν (C-C)	Amorphous
1130	ν_{s} (C-C)	Trans chain
1298	$\tau(CH_2)$	Trans chain
1305	τ (CH_2)	Amorphous

1418	$\delta(CH_2) + \omega(CH_2)$	Crystalline (orthorhombic)
1440	$\delta(CH_2)$	Amorphous trans
1460	$\delta(CH_2)$	Amorphous

[a)] ν, stretching; ν_{as}, anti-symmetric stretching; ν_s, symmetric stretching; τ, twisting; δ, bending, ω, wagging.

The changes of the mass fractions of the chains in various phases with time are shown in Fig. 4. The crystallinity of the LDPE specimen remains almost constant in the early stage, followed by an increase at 600 h. The crystallinity after 1080 h irradiation reaches 0.60, which is as high as the typical value for HDPE. The stepwise increase in the crystallinity at 600 h was confirmed by wide-angle X-ray diffraction (WAXD) and density measurements (see Figs. S-2 and S-6 in the Supporting Information). Moreover, a similar temporal change in the crystallinity has been observed by solid-state NMR spectroscopy during thermal degradation of HDPE [46]. An increase in the crystallinity has also been reported during degradation of PEs under various conditions [29,30,21,47]. The ratios of the intensities of several Raman bands have been used as

spectroscopic markers for wear of ultra-high molecular-weight polyethylene [48]. The sharp increase in the crystallinity at 600 h is explained by the chemicrystallization process [9,10], because a decrease in the molecular weight occurs at the same time.

According to small-angle X-ray scattering (SAXS) measurements, decreases in the amorphous thickness and long period are observed at 600 h (see Fig. S-5 in the Supporting Information). Therefore, the thinning of the amorphous layer at 600 h can be interpreted as a consequence of the increase in the crystallinity. Considering that the increase in the crystallinity leads to macroscopic shrinkage of the specimen, it is likely that the surface crack formation after 840 h is triggered by chemicrystallization.

As shown in Fig. 4, the mass fraction of NCCT chains sharply decreases at 600 h, while the mass fractions of trans and amorphous chains gradually increase and decrease from 420 h, respectively. This suggests that conversion of NCCT chains to crystalline chains is important for chemicrystallization. The fractions of the crystalline, amorphous and interphase phases of the three-phase model [36] has been determined from the Raman spectra of photodegraded polyethylene [27]. They have reported an increase in the crystallinity and decreases in the amorphous and interphase phases during the

photodegradation. The present results are consistent with their results, though the irradiation time dependences seem to be monotonous and the relation to the structural changes has not been shown in their publication. The changes of the intensities of the 1063 and 1130 cm^{-1} bands with time are shown in Fig. 5. The intensities of these bands gradually increase with increasing exposure time, suggesting an increase in the mass fraction of consecutive (n > 10) trans chains. Considering that the fraction of trans chains essentially remains constant in the early stage before 460 h, the increase in the mass fraction of consecutive trans chains is explained by an increase in the length of the short trans chains. The intensities of these two bands markedly decrease after chemicrystallization at 600 h, indicating a decrease in the mass fraction of short trans chains after the sharp increase in the crystallinity.

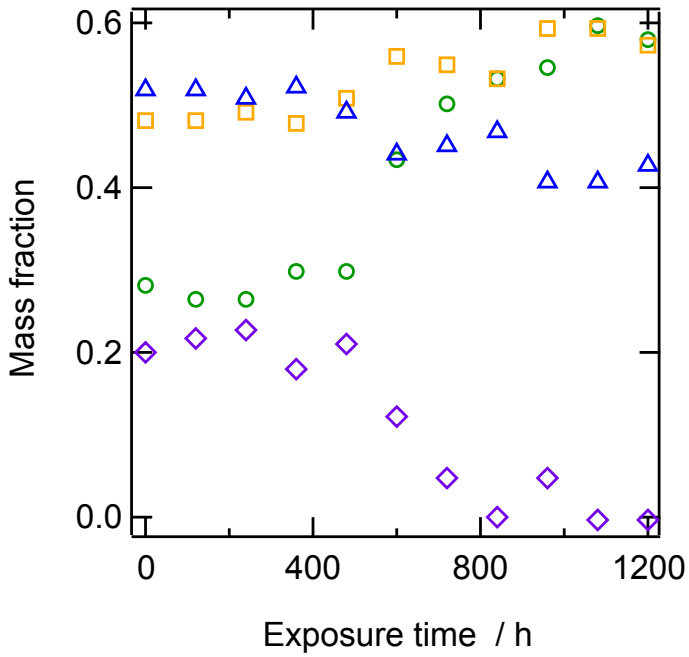

Fig. 4 Changes of the crystallinity (circles) and mass fractions of trans (squares), amorphous (triangles), and NCCT (diamond) chains with UV exposure time.

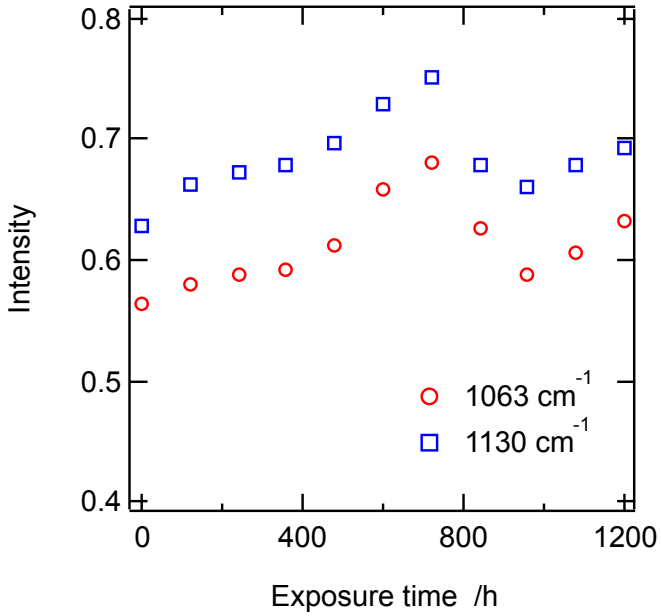

Fig. 5 Changes of the intensities of the 1063 (circles) and 1130 cm^{-1} (squares) bands with UV exposure time.

The peak shifts calculated using Eq. (1) are plotted as a function of the UV exposure time in Fig. 6. The 1063 and 1130 cm^{-1} bands assigned to the C–C stretching modes of the trans chains show gradual red shifts, suggesting that stretching stress is applied to the consecutive ($n > 10$) trans chains [35] during the entire UV exposure test. The C–C stretching mode of the amorphous chain at 1080 cm^{-1} shows a blue shift, suggesting that compression stress is applied to the amorphous phase. The compression on the amorphous chains is consistent with the gradual blue shifts of the 1440 and 1460 cm^{-1} bands, which is interpreted as CH_2 motion in the amorphous phase becoming more restricted [49] at longer UV irradiation time. These Raman spectral shifts suggest that the morphological changes are induced by UV irradiation, which affects the conformation and load sharing, even in the early stage of LDPE photodegradation.

The microscopic stress has been evaluated from the Raman peak shifts for highly-drawn specimens [50-52], where the peak shifts are simply induced by the external stress owing to the absence of the plastic deformation. By using their peak shift coefficients [50-52], the stretching stress along and perpendicular to the molecular axis could be estimated to be 70-100 and 25-50 MPa, respectively. The rough estimation of

the compression stress on the amorphous chains from the peak shifts of the 1440 and 1460 cm^{-1} bands would give 50-250 and 70 MPa, respectively. These values seem to be appreciably overestimated, because the peak shifts are also affected by the microscopic structural and morphological changes caused by photodegradation. In fact, the peak shifts remain the levels even after the surface crack formation after 840 h, which would result in release of the internal stress.

The crystalline 1418 cm^{-1} band shows a red shift after 600 h, indicating contraction of the *ab* plane of the orthorhombic crystal [53], which is confirmed by WAXD analysis (see Fig. S-3 in the Supporting Information). Thus, chemicrystallization is accompanied by a decrease of the interchain distance. Although the increase in the crystallinity at ~600 h is expected to result in thickening of the crystalline thickness, the experimental values determined by SAXS measurements (see Fig. S-5 in the Supporting Information) remain essentially constant during the entire photodegradation process, suggesting that the thickening of the crystalline layer owing to the increase in the crystallinity is canceled out by contraction of the crystalline lattice.

Considering that the crystalline structures show only the slight decrease in the

interchain distance, the appreciable shifts of the amorphous bands at 1440 and 1460 cm^{-1} suggest that the photodegradation preferentially proceeds in the amorphous phase. The importance of the amorphous phase is supported by the fact that the amorphous thickness appreciably decreases with the exposure time, whereas the crystalline thickness remains practically the same, which has also been reported in the literatures [10-12].

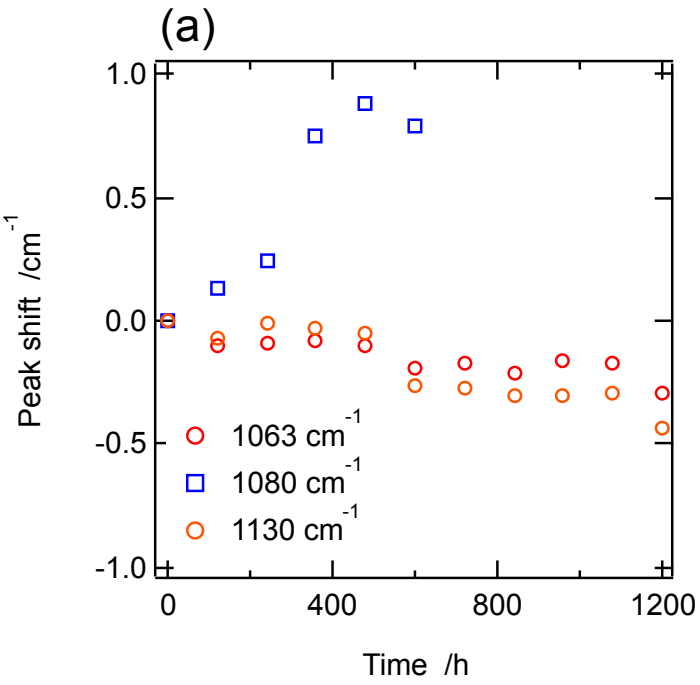

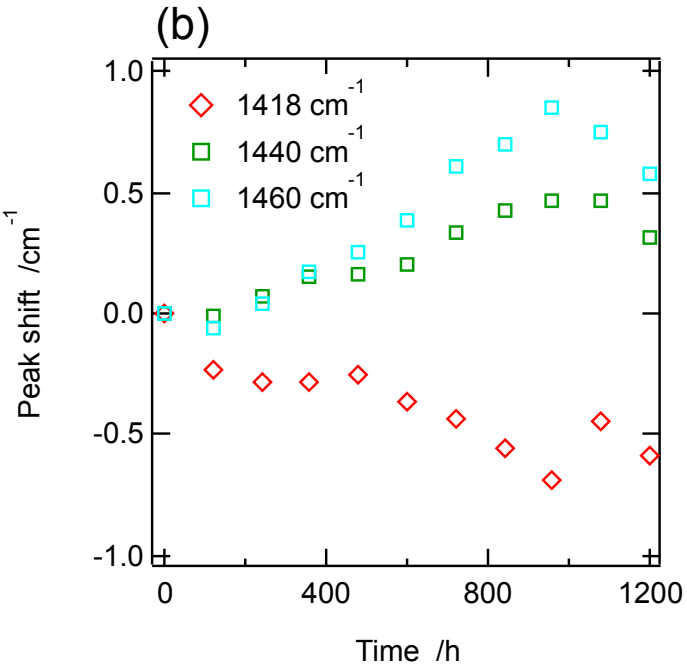

Fig. 6 Changes of the peak shifts of the (a) C–C stretching and (b) CH_2 bending modes with UV exposure time.

The fraction of consecutive (n > 10) trans chains increases with increasing exposure time in the early stage before 480 h, while the fraction of trans chains remains constant. It is plausible that formation of consecutive trans chains in the amorphous phase leads to suppression of the chain mobility, as observed in the blue shifts of the 1440 and 1460 cm^{-1} bands. When the concentration of consecutive trans chains exceeds a critical value, chemicrystallization may occur, resulting in an increase in the crystallinity and shrinking of the *ab* plane at ~600 h. Chemicrystallization is likely to induce

macroscopic shrinkage of the specimens, leading to surface cracks and embrittlement.

4. Conclusions

Raman spectroscopy has revealed the morphological changes during LDPE degradation at the molecular level. In the early stage of photodegradation, short trans chains become longer and are converted to consecutive trans chains ($n > 10$). During the increase in the number of consecutive trans chains, stretching and compression stresses are applied to the consecutive trans and amorphous chains, respectively. An increase in crystallinity occurs at 600 h, accompanied by denser stacking of the crystalline chains and thinning of the amorphous layer. Shrinkage of the specimen leads to formation of surface cracks, which accelerates embrittlement of the specimens. Because these changes are also observed in the early stage before chemicrystallization, the present spectroscopic technique is a non-destructive and non-contact method for evaluating degradation of polymeric materials. For evaluation of the microscopic stress and structural changes during degradation, further experiments and analyses are now in progress for PE with various primary and super- structures.

Acknowledgments

We thank Mr. Y. Yonezawa (Adeka Corp.) for performing the UV exposure tests. We thank Mr. Y. Tsuchida (Northeastern Industrial Research Center of Shiga Prefecture) for performing the HT-GPC measurements and analyses. This work was financially supported by KAKENHI (grant number 16K14456) and JSPS Research Fellowships for Young Scientists (grant number 16J00528). We thank Edanz Group (www.edanzediting.com/ac) for editing a draft of this manuscript.

References

[1] White JR, Turnbull A. Weathering of polymers: mechanisms of degradation and stabilization, testing strategies and modelling. J Mater Sci 1994;29:584–613. doi:10.1007/BF00445969.

[2] Sedlar J, Marchal J, Petruj J. Photostabilising mechanisms of HALS: A critical review. Polymer Photochemistry 1982;2:175–207. doi:10.1016/0144-2880(82)90026-4.

[3] Allen NS, Chirinis-Padron A, Henman TJ. The photo-stabilisation of polypropylene: A review. Polym Degrad Stab 1985;13:31–76. doi:10.1016/0141-3910(85)90133-8.

[4] Hamid SH. Handbook of Polymer Degradation. 2nd ed. New York: Marcel Dekker; 2000. doi:0824703243.

[5] Rivaton A, Gardette JL, Mailhot B, Morlat Therlas S. Basic Aspects of Polymer Degradation. Macromol Symp 2005;225:129–46. doi:10.1002/masy.200550711.

[6] Celina M, Gillen KT, Assink RA. Accelerated aging and lifetime prediction: Review of non-Arrhenius behaviour due to two competing processes. Polym Degrad Stab 2005;90:395–404. doi:10.1016/j.polymdegradstab.2005.05.004.

[7] White JR. Polymer ageing: physics, chemistry or engineering? Time to reflect. Comptes Rendus Chimie 2006;9:1396–408. doi:10.1016/j.crci.2006.07.008.

[8] Gauthier E, Laycock B, Cuoq FJJM, Halley PJ, George KA. Correlation between chain microstructural changes and embrittlement of LLDPE-based films during photo- and thermo-oxidative degradation. Polym Degrad Stab 2013;98:425–35. doi:10.1016/j.polymdegradstab.2012.08.021.

[9] Fayolle B, Colin X, Audouin L, Verdu J. Mechanism of degradation induced embrittlement in polyethylene. Polym Degrad Stab 2007;92:231–8. doi:10.1016/j.polymdegradstab.2006.11.012.

[10] Fayolle B, Richaud E, Colin X, Verdu J. Review: degradation-induced embrittlement in semi-crystalline polymers having their amorphous phase in rubbery state. J Mater Sci 2008;43:6999–7012. doi:10.1007/s10853-008-3005-3.

[11] Hsu Y-C, Weir MP, Truss RW, Garvey CJ, Nicholson TM, Halley PJ. A fundamental study on photo-oxidative degradation of linear low density polyethylene films at embrittlement. Polymer 2012;53:2385–93. doi:10.1016/j.polymer.2012.03.044.

[12] Hsu Y-C, Truss RW, Laycock B, Weir MP, Nicholson TM, Garvey CJ, Halley PJ. The effect of comonomer concentration and distribution on the photo-oxidative degradation of linear low density polyethylene films. Polymer 2017;119:66–75. doi:10.1016/j.polymer.2017.05.020.

[13] Celina MC. Review of polymer oxidation and its relationship with materials performance and lifetime prediction. Polym Degrad Stab 2013;98:2419–29. doi:10.1016/j.polymdegradstab.2013.06.024.

[14] Liu M, Horrocks AR, Hall ME. Correlation of physicochemical changes in UV-exposed low density polyethylene films containing various UV stabilisers. Polym Degrad Stab 1995;49:151–61. doi:10.1016/0141-3910(95)00036-L.

[15] Briassoulis D, Aristopoulou A, Bonora M, Verlodt I. Degradation Characterisation of Agricultural Low-density Polyethylene Films. Biosystems Engineering 2004;88:131–43. doi:10.1016/j.biosystemseng.2004.02.010.

[16] Dilara PA, Briassoulis D. Degradation and Stabilization of Low-density Polyethylene Films used as Greenhouse Covering Materials. Journal of Agricultural Engineering Research 2000;76:309–21. doi:10.1006/jaer.1999.0513.

[17] Dilara PA, Briassoulis D. Standard testing methods for mechanical properties and degradation of low density polyethylene (LDPE) films used as greenhouse covering materials: a critical evaluation. Polymer Testing 1998;17:549–85. doi:10.1016/S0142-9418(97)00074-3.

[18] Winslow FH, Hellman MY, Matreyek W, Stills SM. Autoxidation of semicrystalline polyethylene. Polym Eng Sci 1966;6:273–8. doi:10.1002/pen.760060317.

[19] Gardette JL. Infrared Spectroscopy in the Study of the Weathering and Degradation of Polymers. In: Chalmers JM, editor. Handbook of vibrational spectroscopy, Chichester, UK: John Wiley & Sons, Ltd; 2002. doi:10.1002/0470027320.s6112.

[20] He P, Xiao Y, Zhang P, Zhu N, Zhu X, Yan D. In Situ Fourier transform infrared spectroscopic study of the thermal degradation of isotactic poly(propylene). Appl Spectrosc 2005;59:33–8. doi:10.1366/0003702052940576.

[21] Mellor DC, Moir AB, Scott G. The effect of processing conditions on the u.v. stability of polyolefins. Euro Polym J 1973;9:219–25. doi:10.1016/0014-3057(73)90129-8.

[22] Geetha R, Torikai A, Nagaya S, Fueki K. Photo-oxidative degradation of polyethylene: Effect of polymer characteristics on chemical changes and mechanical properties. Part 1—Quenched polyethylene. Polym Degrad Stab 1987;19:279–92. doi:10.1016/0141-3910(87)90061-9.

[23] Torikai A, Geetha R, Nagaya S, Fueki K. Radiation-induced degradation of polyethylene: Role of amorphous region in the formation of oxygenated products and the mechanical properties. Polym Degrad Stab 1986;16:199–212. doi:10.1016/0141-3910(86)90064-9.

[24] Rouillon C, Bussiere PO, Desnoux E, Collin S, Vial C, Therias S, Gardette JL. Is carbonyl index a quantitative probe to monitor polypropylene

photodegradation? Polym Degrad Stab 2016;128:200–8. doi:10.1016/j.polymdegradstab.2015.12.011.

[25] Ołdak D, Kaczmarek H, Buffeteau T, Sourisseau C. Photo- and Bio-Degradation Processes in Polyethylene, Cellulose and their Blends Studied by ATR-FTIR and Raman Spectroscopies. J Mater Sci 2005;40:4189–98. doi:10.1007/s10853-005-2821-y.

[26] Pezzotti G. Raman spectroscopy of biomedical polyethylenes. Acta Biomater 2017;55:28–99. doi:10.1016/j.actbio.2017.03.015.

[27] Rull F, Rodriguez J, Alia JM, Arroyo F, Edwards H. Evolution of crystallinity in photodegraded polyethylene films studied by ft‐raman spectroscopy. Macromol Symp 1995;94:189–200. doi:10.1002/masy.19950940117.

[28] Taddei P, Tinti A, Fini G. Vibrational spectroscopy of polymeric biomaterials. J Raman Spectrosc 2001;32:619–29. doi:10.1002/jrs.723.

[29] Puppulin L, Miura Y, Casagrande E, Hasegawa M, Marunaka Y, Tone S, Sudo A, Pezzotti G. Validation of a protocol based on Raman and infrared spectroscopies to nondestructively estimate the oxidative degradation of UHMWPE used in total joint arthroplasty. Acta Biomater 2016;38:168–78. doi:10.1016/j.actbio.2016.04.040.

[30] Taddei P, Affatato S, Fagnano C, Bordini B, Tinti A, Toni A. Vibrational spectroscopy of ultra-high molecular weight polyethylene hip prostheses: influence of the sterilisation method on crystallinity and surface oxidation. J Mol Struct 2002;613:121–9. doi:10.1016/S0022-2860(02)00141-2.

[31] Pezzotti G, Takahashi Y, Takamatsu S, Puppulin L, Nishii T, Miki H, et al. Non-destructively Differentiating the Roles of Creep, Wear and Oxidation in Long-Term In Vivo Exposed Polyethylene Cups. Journal of Biomaterials Science, Polymer Edition 2012;22:2165–84. doi:10.1163/092050610X537129.

[32] Medel FJ, Rimnac CM, Kurtz SM. On the assessment of oxidative and microstructural changes after in vivo degradation of historical UHMWPE knee components by means of vibrational spectroscopies and nanoindentation. Journal of Biomedical Materials Research Part A 2009;89:530–8. doi:10.1002/jbm.a.31992.

[33] Kida T, Oku T, Hiejima Y, Nitta K-H. Deformation mechanism of high-density polyethylene probed by in situ Raman spectroscopy. Polymer 2015;58:88–95. doi:10.1016/j.polymer.2014.12.030.

[34] Kida T, Hiejima Y, Nitta KH. Molecular orientation behavior of isotactic polypropylene under uniaxial stretching by rheo-Raman spectroscopy. Express Polym Lett 2016;10:701–9. doi:10.3144/expresspolymlett.2016.63.

[35] Meier RJ. Studying the length of trans conformational sequences in polyethylene using Raman spectroscopy: a computational study. Polymer 2002;43:517–22. doi:10.1016/S0032-3861(01)00416-5.

[36] Strobl GR, Hagedorn W. Raman spectroscopic method for determining the crystallinity of polyethylene. J Polym Sci Polym Phys Ed 1978;16:1181–93. doi:10.1002/pol.1978.180160704.

[37] Migler KB, Kotula AP, Hight Walker AR. Trans-Rich Structures in Early Stage Crystallization of Polyethylene. Macromolecules 2015;48:4555–61. doi:10.1021/ma5025895.

[38] Mutter R, Stille W, Strobl G. Transition Regions and Surface Melting in Partially Crystalline Polyethylene - a Raman-Spectroscopic Study. J Polym Sci Part B: Polym Phys 1993;31:99–105. doi:10.1002/polb.1993.090310113.

[39] Lin W, Cossar M, Dang V, Teh J. The application of Raman spectroscopy to three-phase characterization of polyethylene crystallinity. Polymer Testing 2007;26:814–21. doi:10.1016/j.polymertesting.2007.05.004.

[40] Rull F, Prieto AC, Casado JM, Sobron F, Edwards HGM. Estimation of crystallinity in polyethylene by Raman spectroscopy. J Raman Spectrosc 1993;24:545–50. doi:10.1002/jrs.1250240813.

[41] Ghanbari-Siahkali A, Kingshott P, Breiby DW, Arleth L, Kjellander CK, Almdal K. Investigating the role of anionic surfactant and polymer morphology on the environmental stress cracking (ESC) of high-density polyethylene. Polym Degrad Stab 2005;89:442–53. doi:10.1016/j.polymdegradstab.2005.01.023.

[42] Gall MJ, Hendra PJ, Peacock CJ, Cudby MEA, Willis HA. Laser-Raman spectrum of polyethylene: Part 1. Structure and analysis of the polymer. Polymer 1972;13:104–8. doi:10.1016/S0032-3861(72)80003-X.

[43] Gall MJ, Hendra PJ, Peacock OJ, Cudby MEA, Willis HA. The laser-Raman spectrum of polyethylene. Spectrochimica Acta Part a: Molecular Spectroscopy 1972;28:1485–96. doi:10.1016/0584-8539(72)80118-1.

[44] Bailey RT, Hyde AJ, Kim JJ, McLeish J. Raman studies on oriented, high modulus, polyethylene. Spectrochimica Acta Part a: Molecular Spectroscopy 1977;33:1053–8. doi:10.1016/0584-8539(77)80153-0.

[45] Schachtschneider JH, Snyder RG. Vibrational analysis of the n-paraffins—II. Spectrochimica Acta 1963;19:117–68. doi:10.1016/0371-1951(63)80096-X.

[46] Shi X, Wang J, Stapf S, Mattea C, Li W, Yang Y. Effects of thermo‐oxidative aging on chain mobility, phase composition, and mechanical behavior of high‐density polyethylene. Polym Eng Sci 2011;51:2171–7. doi:10.1002/pen.21988.

[47] Dothée D, Berjot M, Marx J. Measurement of the degree of crystallinity of polyethylene wear debris by means of Raman spectroscopy. Polym Degrad Stab 1988;20:149–55. doi:10.1016/0141-3910(88)90083-3.

[48] Affatato S, Modena E, Carmignato S, Taddei P. The use of Raman spectroscopy in the analysis of UHMWPE uni-condylar bearing systems after run on a force and displacement control knee simulators. Wear 2013;297:781–90. doi:10.1016/j.wear.2012.10.002.

[49] Kida T, Hiejima Y, Nitta K-H. Raman Spectroscopic Study of High-density Polyethylene during Tensile Deformation. Int J Experim Spectrosc Tech 2016;1:1–6.

[50] Tashiro K, Wu G, Kobayashi M, Morphological effect on the Raman frequency shift induced by tensile stress applied to crystalline polyoxymethylene and polyethylene: spectroscopic support for the idea of an inhomogeneous stress distribution in polymer material, Polymer. 1988;29:1768–1778. doi:10.1016/0032-3861(88)90389-8.

[51] Wool RP, Bretzlaff RS, Li BY, Wang CH, Boyd RH, Infrared and raman spectroscopy of stressed polyethylene, J. Polym. Sci. B: Polym. Phys. 1986;24:1039–1066. doi:10.1002/polb.1986.090240508.

[52] Zhao Y, Wang J, Cui Q, Liu Z, Yang M, Shen J, High-pressure Raman studies of ultra-high-molecular-weight polyethylene, Polymer 1990;31:1425–1428. doi:10.1016/0032-3861(90)90145-O.

[53] Otegui J, Vega JF, Martín S, Cruz V, Flores A, Domingo C, Martínez-Salazar J. The unit cell expansion of branched polyethylene as detected by Raman spectroscopy: an experimental and simulation approach. J Mater Sci 2007;42:1046–9. doi:10.1007/s10853-006-1333-8.